Meteorologische Zeitschrift, Vol. **17**, No. 4, 445-453 (August 2008)

Article

Tracking Polar Lows in CLM

MATTHIAS ZAHN[1,2*] and HANS VON STORCH[1,2]

[1] Institute for Coastal Research GKSS Research Center, Geesthacht, Germany
[2] Meteorological Institute University of Hamburg, Hamburg, Germany

(Manuscript received December 3, 2007; in revised form April 18, 2008; accepted April 20, 2008)

Abstract

Polar lows are severe cyclones in sub-polar oceans sized beyond the resolved scale of existing global reanalysis products. We used the NCEP/NCAR reanalyses data to drive a regional climate model (CLM) in order to reproduce finer resolved atmospheric fields over the North Atlantic over a two year period. In these fields we detected polar lows by means of a detection algorithm based on a spatial digital bandpass filter. CLM was run in two different ways, the conventional way and with additionally prescribing the analysed large scale situation. The resulting temporal and spatial distributions of polar lows between the different simulations are compared. A reasonable seasonal cycle and spatial distribution was found for all simulations. A lower number of polar lows in the spectral nudged simulation indicates a closer vicinity to reality. Higher temporal and spatial variability between the conventional simulations suggest a more random generation of polar lows. Frequency distributions of track-lengths reveal shorter tracks when nudging is applied. Maximum wind speeds reveal only minor, insignificant differences between all runs and are higher in conventional mode.

Zusammenfassung

Polar Lows sind Sturmtiefs in subpolaren Meeresgebieten, die unterhalb der Skalen, die in den existierenden globalen Reanalysen noch aufgelöst werden, auftreten. Wir haben ein regionales Klimamodell (CLM) für zwei Jahre mit den globalen NCEP/NCAR Reanalysen angetrieben, um höher aufgelöste atmosphärische Felder über dem Nordatlantik zu erhalten. In den resultierenden Feldern haben wir mit einem Algorithmus, der auf einem räumlichen Band-pass Filter basiert, Polar Lows aufgespürt. Es wurden konventionelle Simulationen mit CLM durchgeführt und außerdem solche, bei denen zusätzlich der großskalige atmosphärische Zustand aus den Reanalysen während der Simulation aufgeprägt wurde ('spektrales Nudging'). Die zeitlichen und räumlichen Verteilungen von Polar Lows aus den verschiedenen Simulationen wurden miteinander verglichen. Eine wirklichkeitsnahe saisonale Verteilung und eine vernünftige räumliche Verteilung wurden in allen Simulationen gefunden. Eine niedrigere Anzahl an Polar Lows in den spektral genudgten Simulationen deutet eine größere Realitätsnähe an. Eine höhere zeitliche und räumliche Variabilität zwischen den konventionell angetriebenen Simulationen weisen auf eine eher zufällige Generierung von Polar Lows hin. Die Häufigkeitsverteilungen der Dauer der Polar Lows ergeben kürzere Zeiten, wenn spektrales Nudging angewendet wird. Die maximalen Windgeschwindigkeiten unterscheiden sich nur geringfügig in allen Simulationen.

1 Introduction

Polar lows are meso-scale sized maritime ground level storms in sub-polar regions. A number of different initial conditions and development mechanisms are thought of being responsible for their development. In general they often form in baroclinic environments (e.g. HARROLD and BROWNING, 1969) or in conjunction with disturbances in the upper levels of the atmosphere (HARROLD and BROWNING, 1969; RASMUSSEN, 1985; BUSINGER, 1985). Often convective processes trigger their development after the initial phase (RASMUSSEN and TURNER, 2003). Conditional instability of the second kind (e.g. RASMUSSEN, 1979) and air sea interaction instability (EMANUEl, 1986; EMANUEL and ROTUNNO, 1989), subsequently renamed Wind Induced Surface Heat Exchange, are the main mechanisms thought of being crucial for the intensification of an induced disturbance.

Due to the Gulf Stream, that causes relatively large differences between the temperature of sea surface and the air above, convective processes in the North Atlantic are favoured and polar lows in this region are especially vigorous. In addition to a couple of model-based case studies (NORDENG and RASMUSSEN, 1991; GRØNÅS and KVAMSTØ, 1995; MAILHOT et al., 1996; NIELSEN, 1997; CLAUD et al., 2004) on the physical processes involved, climatological studies on these meso-scale storms in the North Atlantic have been undertaken by a number of authors applying observational or simulated data (WILHELMSEN, 1985; HAROLD et al., 1999a,b; CONDRON et al., 2006; KOLSTAD, 2006; BRACEGIRDLE and GRAY, 2008). However in the case of using observational data, like e.g. HAROLD et al. (1999a,b), the subjective way of detecting these phenomena suffers from inhomogeneities. Further the restricted investigation period does not enable any statement on long-term statistics of polar low occurrences. This shortcoming also holds for the study by BRACEGIRDLE and GRAY (2008), who detect polar lows in a five year set of numer-

*Corresponding author: Matthias Zahn, Institute for Coastal Research GKSS Research Center Max-Planck Str.1 21502 Geesthacht, Germany

0941-2948/2008/0317 $ 4.05
DOI 10.1127/0941-2948/2008/0317

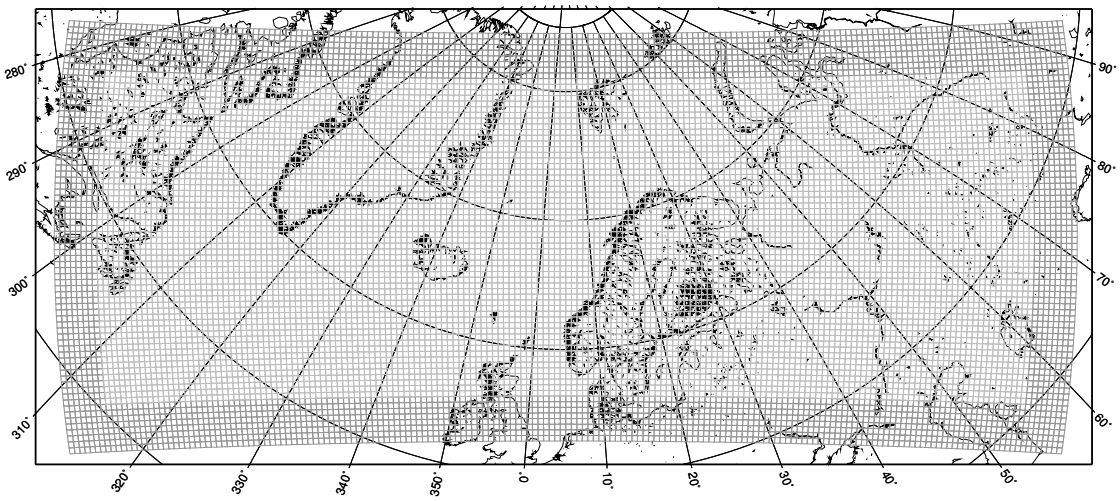

Figure 1: Model grid used for this study. Darker grid boxes at the border represent the sponge zone.

Table 1: Number of retained potential polar lows after applying the respective criteria (confer text). From left to right, the criteria are applied stepwise, e.g. dtz means, that all the requirements to the left also have to be fulfilled.

tracks	filtered minimum	wind speed	dtz	NS direction	no land	supmin
11367	2784	2126	606	160	125	138

ical weather prediction data. Investigations undertaken by CONDRON et al. (2006) or KOLSTAD (2006) consider a long enough time period, but applying relatively coarse gridded global reanalyses they can not resolve individual polar low occurrences.

As a first step to overcome the problem of too short or too coarsely resolved data, ZAHN et al. (accepted) have used CLM (WILL et al., submitted) in conjunction with the NCEP/NCAR (KALNAY et al., 1996) global reanalyses to downscale the large scale state of the atmosphere onto a finer resolution. In three case studies, they investigated the capability of CLM to reproduce polar low occurrences in climate mode. As opposed to the conventional forecast simulations, these climate mode simulations were initiated about two weeks before the polar low developments. Thus the polar lows' dynamical developments are relatively independent from the initial fields and comparable to that in long term simulations.

ZAHN et al. (accepted) compared the performance of two different setups. On the one hand they run CLM in the conventional way, in which the NCEP/NCAR data enters the simulations only at the lateral boundary and via the sea surface temperature. In an other ensemble they additionally applied the spectral nudging methodology of VON STORCH et al. (2000). This mathematical method enforces the upper level large scale state onto CLM during the simulations. Their three investigated cases could be reproduced reliably in ensemble simulations applying spectral nudging. Run in the conventional way CLM was only able to reproduce the cases randomly and also strong variability emerged within the non nudged ensembles.

In this paper we take another step forward towards a comprehensive long term climatology of polar low occurrences in the North Atlantic. Based on the findings of ZAHN et al. (accepted) an algorithm which we think is capable of detecting and tracking polar lows in gridded output data was designed. We applied this detection algorithm onto the output fields of an ensemble of two-year-simulations of the atmospheric state. The resulting outcomes of the ensemble simulations are compared among each other and with climatological studies of other authors.

2 Model Setup and Detection Algorithm

2.1 Setup of CLM

The local area model/regional climate model (LAM/RCM) applied in this study is the CLM, the climate version of the 'Lokal Modell' of the German Weather service. A description of the physics and dynamics of CLM can be found in WILL et al. (submitted). As initial and lateral boundary values, we used the NCEP/NCAR re-analyses (KALNAY et al., 1996) available every six hours with a grid resolution of 2° ($\approx$ 220 km).

Our simulations were run on a rotated grid with 0.44° grid resolution and a longitudinal and latitudinal grid of 184 and 72 points, respectively, and with an integration time step of 240 seconds. The north pole of our rotated geographical grid is located at 175° E and 21.3° N. The simulation area is a rectangle with side lengths

of 8987 km $\times$3516 km (Fig. 1). Regions prone to shallow baroclinic zones along the ice edge, where polar lows often form, are included in the model area.

We conducted four differently set up two-year long simulations with CLM. Two simulations were run the conventional way, namely being constrained only at the lateral boundaries and by the SST and sea ice conditions; these simulations are named 'non-nudged' (CLMnn). In two further simulations we additionally enforced the given upper level large scale state from the NCEP/NCAR data via the spectral nudging procedure developed by (VON STORCH et al., 2000). Spectral nudging is a mathematical method used to enforce a given large scale field during the simulation. Experiments (FESER, 2006) have demonstrated that, while the large-scale circulations are efficiently constrained, the meso-scale variability conditioned by the given large-scale state is not significantly limited by this procedure. Below these nudged simulations are referred to as CLMsn.

The key parameter for spectral nudging is the spectral range, within which the constraint is acting. Here we have chosen zonal wave numbers up to 14 relative to 8987 km and meridional wave numbers up to 5 relative to 3516 km as being constraint (corresponding to a spatial scale of approximately 700 km and more). The constraint is implemented with a vertically growing strength ($\alpha = 0.5$; VON STORCH et al. (2000)) at 850 hPa and above. CLM in this set up was found to reproduce individual polar low occurrences more reliably (ZAHN et al., accepted).

To demonstrate and investigate the variability between the respective simulations, different initial fields were chosen. Two were initiated 1 September 1993 (CLMsn_{09}, CLMnn_{09}) and two further simulations were initiated 1 October 1993 (CLMsn_{10}, CLMnn_{10}).

A simulation period of two years was chosen starting 1 September/October 1993 and finishing 30 September 1995. This period was chosen according to a study by (HAROLD et al., 1999a,b), who counted mesocyclones in the North Atlantic by eye in satellite imagery. Further this periods includes two of the three cases investigated in ZAHN et al. (accepted).

2.2 Detection algorithm

Despite the variety of possible forcing mechanisms polar lows of all origin have in common that they, by definition, are disturbances on the meso-scale. To closer investigate the models' behaviour on these scales ZAHN et al. (accepted) successfully applied a near isotropic digital bandpass filter to extract the meso-scale parts in the mean sea level pressure (mslp) fields. Thereby the polar lows became more distinctive and showed up as minima in the filtered mslp fields. We exploit this in the first step of our detection procedure and, as a first step, separate the meso-scale from the full three hourly mslp fields of the CLM simulations.

We used a near isotropic bandpass filter as described by FESER and VON STORCH (2005) with the same configuration as ZAHN et al. (accepted). They approximated the response function $\kappa(k^*) = 0$ for all $k^* \leq 6, \kappa(k^*) = 1$ for all $k^* \in [8, 15]$, and $\kappa(k^*) = 0$ for all $k^* \geq 18$ with a footprint of 21×21 grid points and the two-dimensional wave number k^*. That is, phenomena on scales larger than approximately $\frac{3516}{6}\text{km} \approx 600$ km and smaller than approximately $\frac{3516}{18}\text{km} \approx 200$ km are filtered out, while scales between 230 km and 450 km are to first order retained. All the positions of the minima in the spatial band pass filtered output mslp fields falling below –1 hPa are stored.

In a second step, these detected positions are combined to individual tracks assuming a maximum propagation speed of 67 $\frac{\text{km}}{h}$. This value is sufficient to catch polar lows with a typical propagation speed of 15–25 kts (27.8–46.3 $\frac{\text{km}}{h}$) as empirically found by (NOER and OVHED, 2003). It is also above the maximum propagation speed of 35 kts (65 $\frac{\text{km}}{h}$) found for most of the polar lows in (WILHELMSEN, 1985). If there is another position fulfilling the requirements of the first step in the next stored time step (3 hrs) within a distance of approximately 200 km, both are merged to one individual track and so on. In the case of two or more filtered minima in the next time step, only the closer one is assigned to the currently treated track.

Applied to CLMsn_{09} this procedure returns 11367 individual tracks of potential polar lows from October 1993 through September 1995. As this number obviously is much too high, further criteria are requested. Therefore, in a third step, further constraints are inspected along the individual tracks. Principally, these constrains can be checked individually and the respective threshold values can be altered. In the following, we apply them step by step in an additive way, i.e. when a new constraint is introduced, those treated before still have to be fulfilled.

Filtered minimum

Polar lows are strong meso-scale disturbances. In order to only retain the stronger ones, we exclude those tracks, whose minima do not fall below a value of –2 hPa at least once. The 'adhoc' threshold of –2 hPa has been chosen based on the work by ZAHN et al. (accepted). The three investigated polar cases in their study do all fall below this value. The implementation of this constraint dismisses approximately 75 % and leaves 2784 of the potential polar lows (Tab. 1).

Wind speed

Polar lows come along with strong surface wind speeds. A commonly used requirement for meso-scale cyclones to be classified as polar lows is a surface wind speed near or above gale force (RASMUSSEN and TURNER, 2003). We check the 10 m wind speed along our tracks

and demand, that the modelled maximum 10 m wind speed in a distance of about 100 km around the localised minimum must exceed 13.9 $\frac{m}{s}$ at at least 20 % of the positions. This and the 'filtered minimum' constraint applied only leave 2126 potential polar low positions.

Vertical stability (dtz)

In general polar lows are convectively triggered systems. In a convectively unstable atmosphere, the temperature in the lower levels is warmer than in the levels above. To implement a preferably easy vertical stability criterion the temperature difference between the sea surface temperature (SST) and the 500 hPa (T_{500}) must exceed 43°C at least once along the track. The value was chosen following the threshold for favourable conditions for polar lows to develop used at the Norwegian Meteorological Institute (NOER and OVHED, 2003). After additionally applying this criterion, only 606 potential polar lows are retained.

North South direction

A further requirement is a southward moving track, i.e. the first detected position has to be about 100 km ($\approx 1°$) farther north than the last. There are two reasons for the implementation of this criterion. We often found synoptic systems with a meso-scale contribution in their centre. In the North Atlantic these systems usually propagate from lower latitudes northward and are thus excluded. The second reason is that polar lows usually occur during cold air outbreaks, in which they usually take a southward track. Now only 160 potential polar lows are left. Note that this criterion inhibits the possibility of single sighted polar lows and that some polar lows at least in the Labrador Sea or in the area east of Greenland falsely might be excluded.

No land

This is a more technical constraint. As shown by ZAHN et al. (accepted) the filtering procedure can be influenced by mountainous orography along coastlines. This led to a couple of supposedly falsely identified disturbances. To avoid these 'artificial' polar lows, detected tracks taking paths along the model's coastal grid boxes in more than 50 % of their time are dismissed, leaving 125 tracks.

Very strong filtered minimum (supmin)

However if the filtered minimum falls below –6 hPa at least once along the track and additionally, the 'no land' criterion is fulfilled, a very strong meso-scale disturbance is assumed and the other constraints are overridden. This leads to the final number of 138 detected polar lows within two years.

2.3 Exemplary verification of the detection algorithm

A comprehensive verification of our setup to detect polar lows would require two different procedures. On the one hand a demonstration would be needed, that a given polar low's position in the CLM output fields is detected and non polar low positions are not. On the other hand a validation would be needed, that an occurred polar low is indeed reproduced by CLM. An extensive case to case validation of the latter is not possible due to a lacking comprehensive data base of observed polar lows. Our original intent to compare with HAROLD et al. (1999a,b) was not appropriate, because they did not only count polar lows, but all meso-cyclonic cloud structures without any further constraints, more than 4000 altogether.

Here we exemplary show, that we successfully were able to reproduce and detect the tracks of the two polar lows from ZAHN et al. (accepted). These are plotted in Fig. 2. The first case appeared on 14 October 1993 south of Spitsbergen and decayed at the southern Norwegian coast on the 16th after taking a southward track over the Atlantic (NIELSEN, 1997; CLAUD et al., 2004; BRACEGIRDLE and GRAY, 2006). In our simulations this case is detectable already in the morning of the 13th. It lasts until the 16th, but the meso-scale minimum does not reach the Norwegian coast.

The second case developed on 8 December 1993 southwest of Iceland in connection with a 500 hPa upper level cold core vortex southwest of Iceland (RASMUSSEN and TURNER, 2003). This polar low also has successfully been reproduced and detected even after a simulation period of more than three months (Fig. 2).

Beyond a case to case validation, a climatological validation can also be sufficient for the application of models in climate issues. It could be possible, that individual events are not caught correctly by the model, but the statistics are similar to observational evidence, anyway. In the following we show, that the climatological outcomes of our set up are close to what work by other authors has been resulted in.

3 Results

In this chapter we first present the temporal distribution and then the spatial distribution of detected polar low occurrences in CLMsn as well as in CLMnn. Finally also frequency distributions of track lengths and 10 m maximum wind speeds are shown.

3.1 Temporal distribution

Polar lows are winter phenomena. In previous studies (WILHELMSEN, 1985; LYSTAD, M., 1986; NOER and OVHED, 2003) for the northern North Atlantic region, polar low activity was found to normally begin in October and having a peak in December/January. After

Table 2: Number of detected polar low cases in the simulations in conventional mode initialised Sep 1993 ($CLMnn_{10}$) and Oct 1993 ($CLMnn_{09}$) and in spectral nudging mode initialised Sep 1993 ($CLMsn_{10}$) and Oct 1993 ($CLMsn_{09}$) and number of tracks with at least one counterpart in any of the other runs. Counterparts are defined according to the following conditions: a) Two tracks occupy the same position at the same time at least once (strict criterion). b) At least one position of track two is within a diameter of 250 km of any position of track one within a time interval of $\pm$ 3 hours (less restrictive criterion).

a) identical position

	cases	$CLMsn_{09}$	$CLMsn_{10}$	$CLMnn_{09}$	$CLMnn_{10}$
$CLMsn_{09}$	138	-	77	9	5
$CLMsn_{10}$	146	76	-	7	4
$CLMnn_{09}$	169	9	7	-	27
$CLMnn_{10}$	164	5	4	27	-

b) deviations in time and position allowed

	cases	$CLMsn_{09}$	$CLMsn_{10}$	$CLMnn_{09}$	$CLMnn_{10}$
$CLMsn_{09}$	138	-	101	46	44
$CLMsn_{10}$	146	101	-	47	45
$CLMnn_{09}$	169	47	48	-	86
$CLMnn_{10}$	164	45	45	87	-

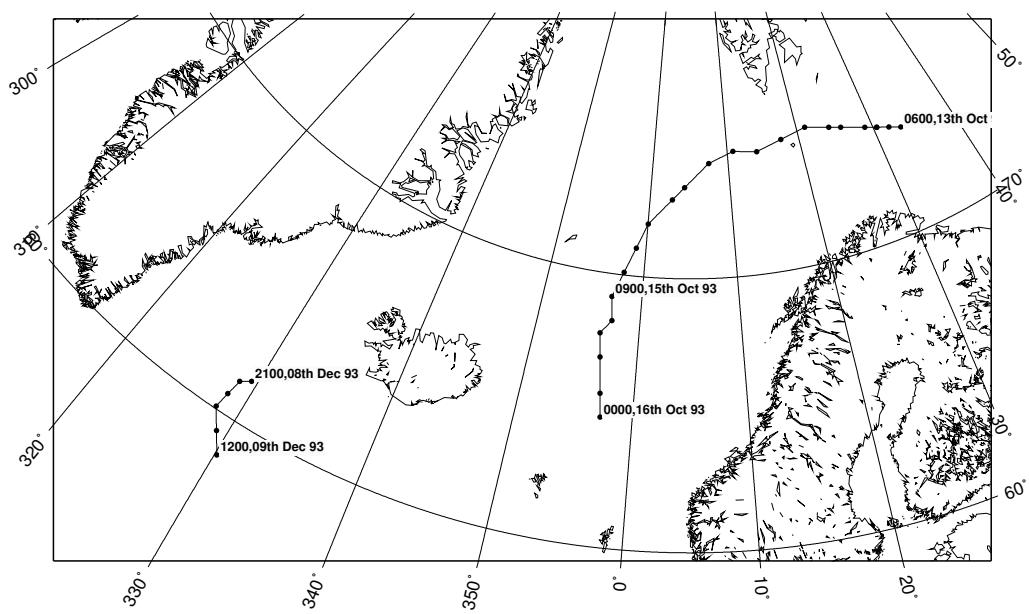

Figure 2: Detected tracks of polar lows investigated in ZAHN et al. (accepted).

a minimum of activity in February, a second peak turns out in March. From June on, polar lows are not likely to occur any more. We find a qualitatively similar situation here (Fig. 3). In the spectrally nudged as well as in the two conventional runs, no polar lows are detected between June and August. The maximum monthly number of detected polar lows in all simulations is found in January in the first winter. In the second winter, $CLMsn_{09}$ reveals slightly more polar lows in March than in January. Apart from $CLMnn_{10}$ in the first winter season, these January maxima are always followed by a minimum in February and a second peak in March according to the mentioned studies.

Comparison between the two different setups reveals a higher number of detected cases in the conventional runs, 169 in $CLMnn_{09}$ and 164 in $CLMnn_{10}$. These numbers are about 12 % to 22 % higher than the numbers of 138 detected cases in $CLMsn_{09}$ and 146 in $CLMsn_{10}$ (Tab. 2).

A total number of 4054 individual cyclones was found by HAROLD et al. (1999a). However they considered all mesocyclones without further conditions and not just

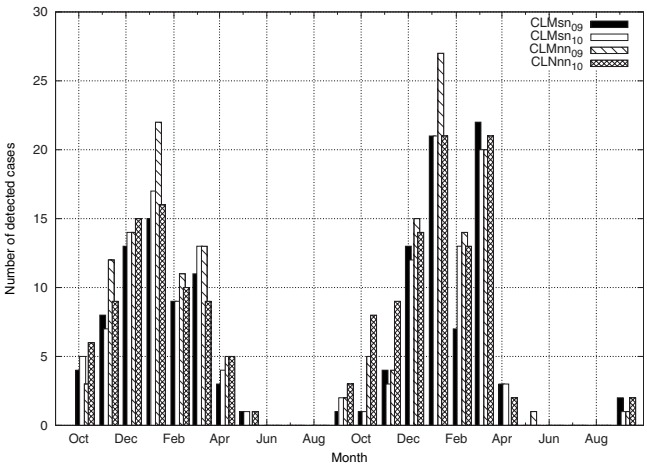

Figure 3: Polar low frequency distribution October 1993 until September 1995.

polar lows and thus this number cannot act as a quantitative reference. Focusing exclusively on gale producing polar lows, (WILHELMSEN, 1985) in times of much sparser observational coverage found 33 cases within 5 years, LYSTAD, M. (1986) 79 in a three year period and NOER and OVHED (2003) made out 41 polar lows within 4 winters. Still a quantitative comparison is inappropriate, as these studies only where conducted for a smaller sub-region of our model domain, the northern North Atlantic. Further, different time periods were considered and different criteria for polar lows were applied. For instance, NOER and OVHED (2003) demand a wind speed above 17 m/s for a polar low. Anyhow these low numbers slightly suggest a more realistic climatological reproduction of polar low cases in CLMsn.

ZAHN et al. (accepted) found high variability in the conventional simulations for their polar low cases. The same situations holds here. A higher standard deviation of the monthly differences of the number of detected polar lows (cf. Fig. 3) between the conventional simulations ($\sigma_{nn} = 2.52$) compared to the nudged simulations ($\sigma_{sn} = 1.49$) was calculated. This manifests lower variability between the spectrally nudged simulations.

3.2 Spatial distribution

To investigate differences in their spatial distribution, we subdivided our model domain into 14 geographical subregions and counted the number of detected polar lows in each of them. The regions were selected based on the sectioning of HAROLD et al. (1999a) and are referred to with R plus number of region below. However, as mentioned before, we only counted polar lows and not mesocyclones in general and thus an extended comparison with their findings does not seem useful to us. Of each detected track the position with the lowest filtered mslp value was used and it is assumed, that this position of the strongest meso-scale contribution reflects the simulated mature state. The results are shown in Figure 4.

The maximum number of polar lows is usually found in R5, between Iceland and Greenland. In CLMsn_{09} R5 only holds the second largest number of polar lows behind R10 farther south. However, considering the much smaller maritime area in R5, a larger count density per area unit can be assumed in R5. A maximum in mesocyclonic activity in this region has also been reported by HAROLD et al. (1999a) and by CONDRON et al. (2006). Also BRACEGIRDLE and GRAY (2006), before they solely focus on the Nordic seas neglecting regions west of $5\,^{\circ}$ west, made out a maximum in count density in this region for a four year period, 2000 through 2004. A comparison of count densities of our results would be desirable in subsequent studies, which should closer focus on a comparison between simulation and observation derived climatologies.

Another maximum in polar low activity is usually found between Spitsbergen and Norway. Here, in R2 we have only few polar lows. Possibly, polar lows in this area are shifted to R3 or R7. Further R2 is thought of being a genesis area of polar lows. When plotting the first positions (not shown), the number of polar lows in R2 increases slightly ($+1$) in the nudged simulations and enormously in the conventional ones (up to 11 cases). The same holds for R7, where up to 14/15 polar lows form in the nudged/non nudged simulations.
No polar low activity is found in the Baltic (R14). In the North Sea (R12) 0 to 2 polar lows are found. This is about the order of cases found by AAKJÆR (1992). He found 18 cases in ten winter seasons, with December 1981 being extremely active (7 cases). Often polar lows only enter the North Sea in their decaying stage. The number of detected cases rises to 3/4 detected cases in CLMsn_{09}/CLMsn_{10} and up to 6 cases in CLMnn_{09}, if the tracks' last positions are plotted (not shown). Then, also the Baltic is affected by one polar low in three of the simulations. The same is seen in the region west of Great Britain, R11, where the low number of polar lows increases in the plot of the last positions. Please note that lateral grid boxes in the southern North Sea and in the southern North Atlantic are used in the bandpass filter's footprint and thus can not be considered as potential polar low positions.

The only region, in which the largest and second largest number of polar lows is found in the spectrally nudged runs is R4. Everywhere else (apart from R10) and in accordance with the total numbers of cases, the maximum number of detected polar lows per region is found in one of the conventional simulations. Thereby, their numbers usually differ substantially. Only in the Davies Strait, the numbers are equal. This could be due to the vicinity of the western boundary, where large scale information directly enters the calculations even in the non nudged simulations. As ZAHN et al. (accepted) pointed out, a properly prescribed large scale situation prevents strong variability. The atmospheric properties entering the simulations at its western boundary are usu-

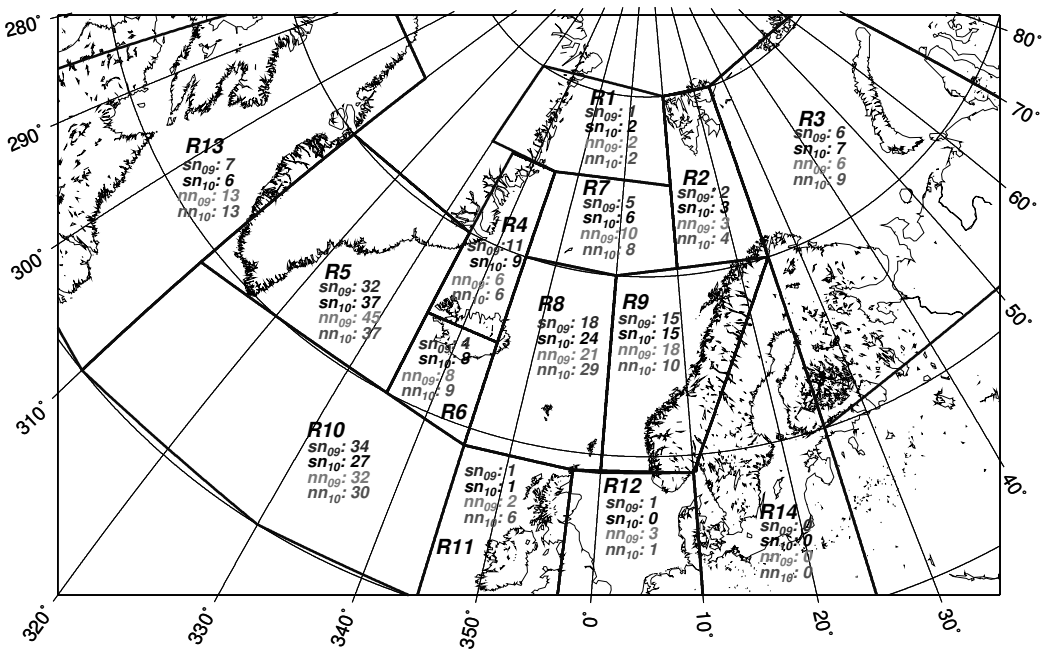

Figure 4: Subregions, for which the number of detected polar lows are counted (R1-R14) and respective number of detected mature state polar lows detected in CLMsn$_{09}$ (sn$_{09}$), CLMsn$_{10}$ (sn$_{10}$), CLMnn$_{09}$ (nn$_{09}$) and CLMnn$_{10}$ (nn$_{10}$). Difference in total number of polar lows (see Tab. 2) and sum of the respective regions is due to polar lows occurring in the Southwest outside the investigated area.

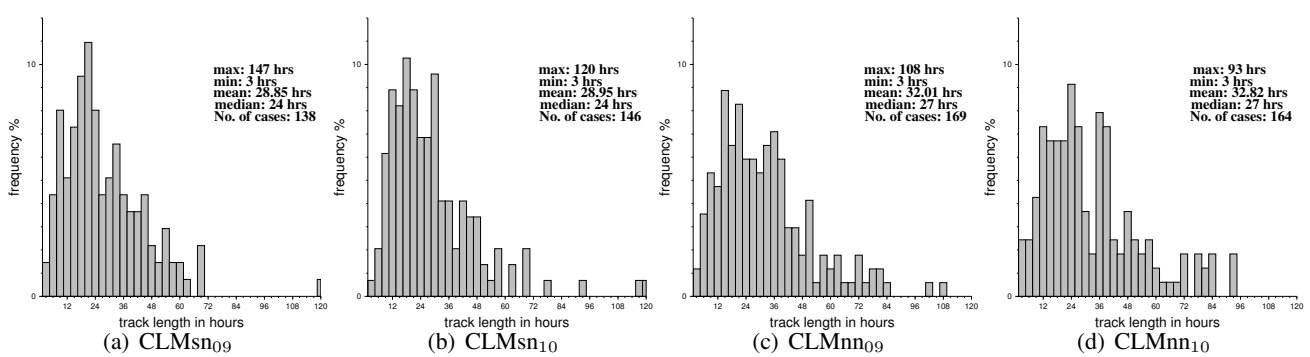

(a) CLMsn$_{09}$ (b) CLMsn$_{10}$ (c) CLMnn$_{09}$ (d) CLMnn$_{10}$

Figure 5: Frequency distribution of detected track lengths in hours.

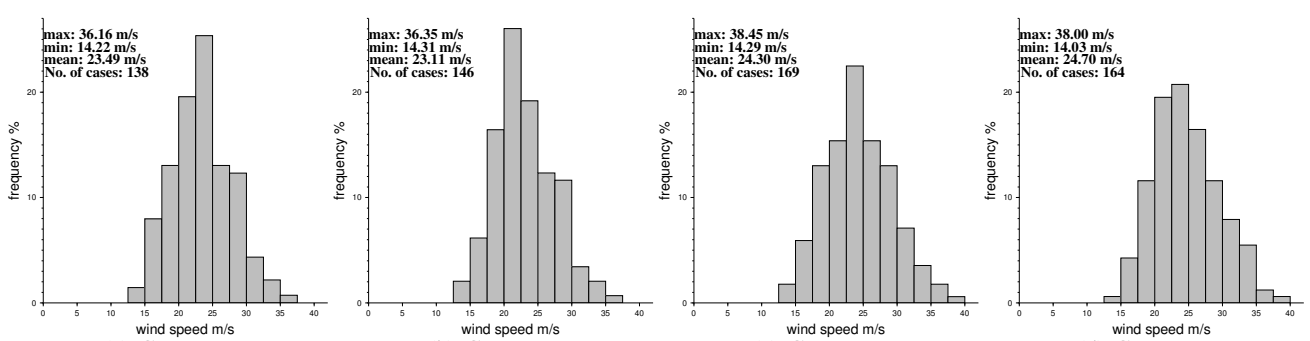

(a) CLMsn$_{09}$ (b) CLMsn$_{10}$ (c) CLMnn$_{09}$ (d) CLMnn$_{10}$

Figure 6: Frequency distribution of maximum wind speed along detected tracks.

ally propagating with the common wind regime in these latitudes from west to east. In regions beyond the influence of the western boundary the situation appears differently. Large variability in the number of polar lows is found. This variability is stronger between the conventional simulations compared to CLMsn and is quantified in a higher standard deviation of the differences in each region in CLMnn ($\sigma_{nn} = 4.06$) compared to CLMsn ($\sigma_{nn} = 3.06$)

To further investigate the differences between the respective runs, we quantified, how many of the detected tracks in one run have a potential counterpart in any of the others (Tab. 2). When a very strict criterion is applied, this number is very low for the comparisons. Only between CLMsn_{09} and CLMsn_{10}, this number is large and almost half of the tracks in one run have a counterpart in the other. Please note, that one track of simulation A can have two counterparts in simulation B, which leads to different numbers in some of the reverse comparisons. When demanding a less restrictive criterion about two thirds of the 'nudged' tracks overlap, whereas this only holds for half of the non nudged.

3.3 Comparison of track-length and wind speed

In this subsection, we investigate the differences in frequency distribution of two parameters characterising the detected features. These are detected track lengths and the respective maximum 10 m wind speeds along the tracks.

The frequency distributions of detected track lengths are shown in Figure 5. The histograms reveal that the polar lows in CLMsn_{09} and CLMsn_{10} are shorter lived than in CLMnn_{09} and CLMnn_{10}. Half of them last for a day or less. The median of track lengths in the conventional simulations is three hours more. The same also holds qualitatively for the mean duration. Reproduced polar lows in the conventional runs last about four hours longer. As polar lows generally are shortly lasting phenomena, the distribution of their track length from the nudged simulations seems to be more realistic.

The 'North South direction' constraint of our tracking algorithm would inhibit track lengths of three hours, namely of only one time step. The three hour bins in Figure 5 are all polar lows, which entered the data base due to the 'very strong filtered minimum' condition, which overrides the others. All of them belong to the same case. This case develops 10 February 1994 in the Atlantic moving northward too quickly for our tracking procedure to be linked to the same track (cf. Page 447). Thus the track is split into several (up to 4) single sighted polar lows.

As discussed before, polar lows already might be detected very early during their development resulting in long tracks. In CLMsn 2/4 tracks of a length of more than three days are figured out and 7/11 in CLMnn. Here it can not be decided whether these are falsely detected polar lows or indeed correctly detected ones. At least the very long tracks of about five days in the nudged simulations seem to be false detections. One of the closer inspected long tracks of CLMnn_{09} consists of several polar lows in the region between Iceland and Greenland, which are merged to one case by the algorithm.

The most severe polar lows in terms of maximum and mean maximum 10 m wind speed (Fig 6) are detected in CLMnn. There are no noticeable differences between the maximum wind speed distributions of all simulations. Unlike in the spatial and temporal distributions, there could no significant differences been detected here. Maxima in the frequency distribution in the order of 20 to 25 m/s are in good accordance with the observed frequency distribution of maximum wind speed in connection with polar lows in WILHELMSEN (1985).

4 Summary and discussion

In this paper we investigated in two-year long simulations with CLM, how the climatology of polar lows is reproduced. Therefore CLM was run with two different setups. On the one hand we conducted two simulations in the conventional way and on the other hand two with additionally prescribing the given large scale situation were arranged. A detection algorithm based on the spatial bandpass filtered mslp fields was developed and applied for the first time to detect individual polar lows. The results of the detection procedure were studied. In our analysis we centred the comparison between the simulations and the variability between the two conventional simulations. Comparisons with other authors' studies are also treated.

In summary, there are no huge temporal or spatial deviations between our results and those from other authors. Overall a seasonal cycle close to what observational evidence points out was detected in all simulations. Spatial distributions seem consistent with other studies.

Fewer polar lows were generated in the nudged simulations and maximum numbers are generated by the non nudged runs. A quantitative difference of more than 10% was found. Maxima in the conventional simulations show up in the number of cases per month as well as in the number of cases per geographical sector. The monthly and regional number of cases in the conventional simulations is subject of higher variability than the number in the spectrally nudged ones. It seems, that the large scale constraint inhibits some of the meso-scale activity, which on the other hand has more freedom to develop in the unconstrained runs. Here, however, this variability seems to be induced randomly. To exclude such random variability, we suggest for a long-term simulation arranged to investigate the 'real' variability, that spectral nudging should be implied.

The frequency of parameters such as detected track lengths and maximum wind speeds only reveal minor,

insignificant differences in general. Track lengths in the nudged simulations are shorter and thus seem to be a little bit more realistic. For a reasonable examination of temporal or spatial differences or trends, the simulated time period is too short. To investigate such long term changes and also differences in different regions will be one of our future tasks in longer lasting simulations. In such simulations we could utilise that our band pass filter detects polar lows independently from their causal mechanisms. This would enable an investigation of the climatology of different processes involved in polar low development, e.g. how often and where polar lows do form in baroclinic environments or in reverse shear conditions.

Acknowledgement

We are thankful to Jonas Bhend for some helpful inputs to the tracking procedure. The work was conducted within the Virtual Institute (VI) EXTROP which is promoted by the "Initiative and Networking Fund" of the Helmholtz Association. NCEP Reanalysis data were provided by the NOAA/OAR/ESRL PSD, Boulder, Colorado, USA, from their Web site at www.cdc.noaa.gov/.

References

AAKJÆR, P. D., 1992: Polar lows affecting Denmark. – Tellus **44A**, 155–172, Doi:10.1034/j.1600-0870.1992.t01-1-00005.x.

BRACEGIRDLE, T., S. GRAY, 2006: The role of convection in the intensification of polar lows. Ph.d. thesis, University of Reading.

—, —, 2008: An objective climatology of the dynamical forcing of polar lows in the Nordic seas. – Int. J. Climatol., published online, DOI: 10.1002/joc.1686.

BUSINGER, S., 1985: The synoptic climatology of polar low outbreaks. – Tellus Series A **37**, 419–432.

CLAUD, C., G. HEINEMANN, E. RAUSTEIN, L. MCMURDIE, 2004: Polar low 'Le Cygne': Satellite observations and numerical simulations. – Quart. J. Roy. Meteor. Soc. **130**, 1075–1102.

CONDRON, A., G. R. BIGG, I. A. RENFREW, 2006: Polar Mesoscale Cyclones in the Northeast Atlantic: Comparing Climatologies from ERA-40 and Satellite Imagery. – Mon. Wea. Rev. **134**, 1518–1533, DOI: 10.1175/MWR3136.1.

EMANUEL, K. A., 1986: An air-sea interaction theory for tropical cyclones. part I: Steady-state maintenance. – J. Atmos. Sci. **43**, 585–605.

EMANUEL, K. A., R. ROTUNNO, 1989: Polar lows as arctic hurricanes. – Tellus **41A**, 1–17.

FESER, F., 2006: Enhanced detectability of added value in limited area model results separated into different spatial scales. – Mon. Wea. Rev. **134**, 2180–2190.

FESER, F., H. VON STORCH, 2005: A spatial two-dimensional discrete filter for limited area model evaluation purposes. – Mon. Wea. Rev. **133**, 1774–1786.

GRØNÅS, S., N. KVAMSTØ, 1995: Numerical simulations of the synoptic conditions and development of arctic outbreak polar lows. – Tellus **47A**, 797–814.

HARROLD, T.W., K.A. BROWNING, 1969: The polar low as a baroclinic disturbance. – Quart. J. Roy. Meteor. Soc. **95**, 710–723.

HAROLD, J. M., G. R. BIGG, J. TURNER, 1999a: Mesocyclone activities over the north-east Atlantic. part 1: Vortex distribution and variability. – Int. J. Climatol. **19**, 1187–1204.

—, —, —, 1999b: Mesocyclone activities over the north-east Atlantic. part 2: An investigation of causal mechanisms. – Int. J. Climatol. **19**, 1283–1299.

KALNAY, E., M. KANAMITSU, R. KISTLER, W. COLLINS, D. DEAVEN, L. GANDIN, M. IREDELL, S. SAHA, G. WHITE, J. WOOLLEN, Y. ZHU, M. CHELLIAH, W. EBISUZAKI, W. HIGGINS, J. JANOWIAK, K. MO, C. ROPELEWSKI, J. WANG, A. LEETMAA, R. REYNOLDS, R. JENNE, D. JOSEPH, 1996: The NCEP/NCAR reanalysis project. – Bull. Amer. Meteor. Soc. **77**, 437–471.

KOLSTAD, E., 2006: A new climatology of favourable conditions for reverse-shear polar lows. – Tellus **58A**, 344–354, DOI: 10.1111/j.1600–0870.2006.00171.x.

LYSTAD, M. (Ed.), 1986: Polar lows in the Norwegian, Greenland and Barents Sea. – Final Rep., Polar Lows Project, The Norwegian Meterological Institute 196 pp.

MAILHOT, J., D. HANLEY, B. BILODEAU, O. HERTZMAN, 1996: A numerical case study of a polar low in the Labrador Sea. – Tellus **48A**, 383–402.

NIELSEN, N., 1997: An early Autumn polar low formation over the Norwegian Sea. – J. Geophys. Res. **102**, 13955–13973.

NOER, G. M. OVHED, 2003: Forecasting of polar lows in the Norwegian and the Barents Sea. – Proc. of the 9th meeting of the EGS Polar Lows Working Group, Cambridge, UK.

NORDENG, T. E. RASMUSSEN, 1991: A most beautiful polar low. A case study of a polar low development in the Bear Island region. – Tellus **44A**, 81–99.

RASMUSSEN, E., 1979: The polar low as an extratropical CISK disturbance. – Quart. J. Roy. Meteor. Soc. **105**, 531–549.

—, 1985: A case study of a polar low development over the Barents Sea. – Tellus **37A**, 407–418.

RASMUSSEN, E. J. TURNER, 2003: Polar Lows: Mesoscale Weather Systems in the Polar Regions. – Cambridge University Press, Cambridge.

VON STORCH, H., H. LANGENBERG, F. FESER, 2000: A spectral nudging technique for dynamical downscaling purposes. – Mon. Wea. Rev. **128**, 3664–3673.

WILHELMSEN, K., 1985: Climatological study of gale-producing polar lows near Norway. – Tellus **37A**, 451–459.

WILL A., M. BALDAUF, B. ROCKEL, A. SEIFERT, submitted: Physics and dynamics of the COSMO-CLM. – Meteorol. Z.

ZAHN, M., H. VON STORCH, S. BAKAN, accepted: Climate mode simulation of North Atlantic Polar Lows in a limited area model. – Tellus A.